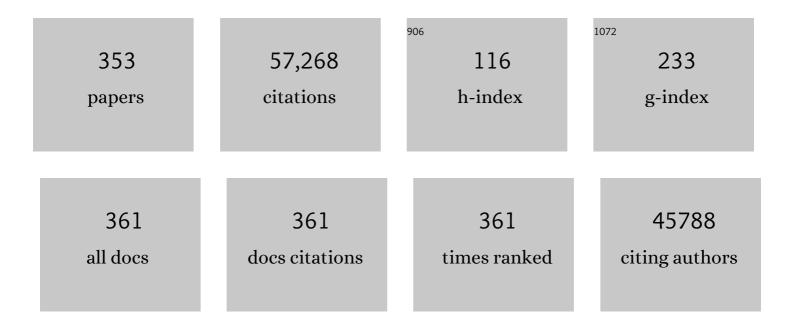
## List of Publications by Year in descending order

Source: https://exaly.com/author-pdf/1060048/publications.pdf Version: 2024-02-01



Διιίλνεν

#	Article	lF	CITATIONS
1	Fully integrated wearable sensor arrays for multiplexed in situ perspiration analysis. Nature, 2016, 529, 509-514.	27.8	3,508
2	Ballistic carbon nanotube field-effect transistors. Nature, 2003, 424, 654-657.	27.8	2,883
3	High-Performance Single Layered WSe <sub>2</sub> p-FETs with Chemically Doped Contacts. Nano Letters, 2012, 12, 3788-3792.	9.1	1,547
4	Nanowire active-matrix circuitry for low-voltage macroscale artificial skin. Nature Materials, 2010, 9, 821-826.	27.5	1,162
5	MoS <sub>2</sub> transistors with 1-nanometer gate lengths. Science, 2016, 354, 99-102.	12.6	1,140
6	User-interactive electronic skin for instantaneous pressure visualization. Nature Materials, 2013, 12, 899-904.	27.5	1,044
7	Three-dimensional nanopillar-array photovoltaics on low-cost and flexible substrates. Nature Materials, 2009, 8, 648-653.	27.5	997
8	Near-unity photoluminescence quantum yield in MoS <sub>2</sub> . Science, 2015, 350, 1065-1068.	12.6	993
9	Strong interlayer coupling in van der Waals heterostructures built from single-layer chalcogenides. Proceedings of the National Academy of Sciences of the United States of America, 2014, 111, 6198-6202.	7.1	970
10	Toward Large Arrays of Multiplex Functionalized Carbon Nanotube Sensors for Highly Sensitive and Selective Molecular Detection. Nano Letters, 2003, 3, 347-351.	9.1	953
11	Wearable sweat sensors. Nature Electronics, 2018, 1, 160-171.	26.0	947
12	High-κ dielectrics for advanced carbon-nanotube transistors and logic gates. Nature Materials, 2002, 1, 241-246.	27.5	928
13	Hysteresis Caused by Water Molecules in Carbon Nanotube Field-Effect Transistors. Nano Letters, 2003, 3, 193-198.	9.1	890
14	Flexible Electronics toward Wearable Sensing. Accounts of Chemical Research, 2019, 52, 523-533.	15.6	713
15	Degenerate n-Doping of Few-Layer Transition Metal Dichalcogenides by Potassium. Nano Letters, 2013, 13, 1991-1995.	9.1	651
16	Air-Stable Surface Charge Transfer Doping of MoS <sub>2</sub> by Benzyl Viologen. Journal of the American Chemical Society, 2014, 136, 7853-7856.	13.7	593
17	Field-Effect Transistors Built from All Two-Dimensional Material Components. ACS Nano, 2014, 8, 6259-6264.	14.6	582
18	Layer-by-Layer Assembly of Nanowires for Three-Dimensional, Multifunctional Electronics. Nano Letters, 2007, 7, 773-777.	9.1	573

#	Article	IF	CITATIONS
19	Autonomous sweat extraction and analysis applied to cystic fibrosis and glucose monitoring using a fully integrated wearable platform. Proceedings of the National Academy of Sciences of the United States of America, 2017, 114, 4625-4630.	7.1	573
20	Strain-Induced Indirect to Direct Bandgap Transition in Multilayer WSe <sub>2</sub> . Nano Letters, 2014, 14, 4592-4597.	9.1	572
21	Polymer Functionalization for Air-Stable n-Type Carbon Nanotube Field-Effect Transistors. Journal of the American Chemical Society, 2001, 123, 11512-11513.	13.7	570
22	Dual-Gated MoS <sub>2</sub> /WSe <sub>2</sub> van der Waals Tunnel Diodes and Transistors. ACS Nano, 2015, 9, 2071-2079.	14.6	560
23	High-Field Quasiballistic Transport in Short Carbon Nanotubes. Physical Review Letters, 2004, 92, 106804.	7.8	543
24	Wafer-Scale Assembly of Highly Ordered Semiconductor Nanowire Arrays by Contact Printing. Nano Letters, 2008, 8, 20-25.	9.1	542
25	Self-Aligned Ballistic Molecular Transistors and Electrically Parallel Nanotube Arrays. Nano Letters, 2004, 4, 1319-1322.	9.1	505
26	Carbon Nanotube Field-Effect Transistors with Integrated Ohmic Contacts and High-κ Gate Dielectrics. Nano Letters, 2004, 4, 447-450.	9.1	498
27	MoS <sub>2</sub> P-type Transistors and Diodes Enabled by High Work Function MoO <sub><i>x</i></sub> Contacts. Nano Letters, 2014, 14, 1337-1342.	9.1	487
28	Preferential Growth of Semiconducting Single-Walled Carbon Nanotubes by a Plasma Enhanced CVD Method. Nano Letters, 2004, 4, 317-321.	9.1	485
29	A Wearable Electrochemical Platform for Noninvasive Simultaneous Monitoring of Ca <sup>2+</sup> and pH. ACS Nano, 2016, 10, 7216-7224.	14.6	480
30	Optically- and Thermally-Responsive Programmable Materials Based on Carbon Nanotube-Hydrogel Polymer Composites. Nano Letters, 2011, 11, 3239-3244.	9.1	476
31	Hole Selective MoO <sub><i>x</i></sub> Contact for Silicon Solar Cells. Nano Letters, 2014, 14, 967-971.	9.1	476
32	Efficient silicon solar cells with dopant-free asymmetric heterocontacts. Nature Energy, 2016, 1, .	39.5	461
33	High Performance n-Type Carbon Nanotube Field-Effect Transistors with Chemically Doped Contacts. Nano Letters, 2005, 5, 345-348.	9.1	453
34	Direct Chemical Vapor Deposition of Graphene on Dielectric Surfaces. Nano Letters, 2010, 10, 1542-1548.	9.1	439
35	Wearable Microfluidic Diaphragm Pressure Sensor for Health and Tactile Touch Monitoring. Advanced Materials, 2017, 29, 1701985.	21.0	431
36	Enabling unassisted solar water splitting by iron oxide and silicon. Nature Communications, 2015, 6, 7447.	12.8	429

#	Article	IF	CITATIONS
37	Germanium nanowire field-effect transistors with SiO2 and high-κ HfO2 gate dielectrics. Applied Physics Letters, 2003, 83, 2432-2434.	3.3	424
38	Ballistic Transport in Metallic Nanotubes with Reliable Pd Ohmic Contacts. Nano Letters, 2003, 3, 1541-1544.	9.1	416
39	2D materials advances: from large scale synthesis and controlled heterostructures to improved characterization techniques, defects and applications. 2D Materials, 2016, 3, 042001.	4.4	408
40	Ultra-high-yield growth of vertical single-walled carbon nanotubes: Hidden roles of hydrogen and oxygen. Proceedings of the National Academy of Sciences of the United States of America, 2005, 102, 16141-16145.	7.1	403
41	A biomimetic eye with a hemispherical perovskite nanowire array retina. Nature, 2020, 581, 278-282.	27.8	392
42	Passivating contacts for crystalline silicon solar cells. Nature Energy, 2019, 4, 914-928.	39.5	374
43	Ultrathin compound semiconductor on insulator layers for high-performance nanoscale transistors. Nature, 2010, 468, 286-289.	27.8	373
44	Fully Printed, High Performance Carbon Nanotube Thin-Film Transistors on Flexible Substrates. Nano Letters, 2013, 13, 3864-3869.	9.1	372
45	Printed Carbon Nanotube Electronics and Sensor Systems. Advanced Materials, 2016, 28, 4397-4414.	21.0	369
46	Polarization-resolved black phosphorus/molybdenum disulfide mid-wave infrared photodiodes with high detectivity at room temperature. Nature Photonics, 2018, 12, 601-607.	31.4	366
47	Toward the Development of Printable Nanowire Electronics and Sensors. Advanced Materials, 2009, 21, 3730-3743.	21.0	363
48	Silicon heterojunction solar cell with passivated hole selective MoOx contact. Applied Physics Letters, 2014, 104, .	3.3	363
49	Diameter-Dependent Electron Mobility of InAs Nanowires. Nano Letters, 2009, 9, 360-365.	9.1	353
50	Carbon Nanotube Transistor Arrays for Multistage Complementary Logic and Ring Oscillators. Nano Letters, 2002, 2, 929-932.	9.1	325
51	Controlled nanoscale doping of semiconductors via molecular monolayers. Nature Materials, 2008, 7, 62-67.	27.5	311
52	Goldâ€Mediated Exfoliation of Ultralarge Optoelectronicallyâ€Perfect Monolayers. Advanced Materials, 2016, 28, 4053-4058.	21.0	307
53	Solution-Synthesized High-Mobility Tellurium Nanoflakes for Short-Wave Infrared Photodetectors. ACS Nano, 2018, 12, 7253-7263.	14.6	298
54	Wearable Microsensor Array for Multiplexed Heavy Metal Monitoring of Body Fluids. ACS Sensors, 2016, 1, 866-874.	7.8	297

#	Article	IF	CITATIONS
55	Extremely Bendable, High-Performance Integrated Circuits Using Semiconducting Carbon Nanotube Networks for Digital, Analog, and Radio-Frequency Applications. Nano Letters, 2012, 12, 1527-1533.	9.1	292
56	A Wearable Microfluidic Sensing Patch for Dynamic Sweat Secretion Analysis. ACS Sensors, 2018, 3, 944-952.	7.8	285
57	High-Gain Inverters Based on WSe <sub>2</sub> Complementary Field-Effect Transistors. ACS Nano, 2014, 8, 4948-4953.	14.6	284
58	Carbon nanotube electronics – moving forward. Chemical Society Reviews, 2013, 42, 2592-2609.	38.1	276
59	Roll-to-Roll Gravure Printed Electrochemical Sensors for Wearable and Medical Devices. ACS Nano, 2018, 12, 6978-6987.	14.6	275
60	Carbon Nanotube Active-Matrix Backplanes for Conformal Electronics and Sensors. Nano Letters, 2011, 11, 5408-5413.	9.1	270
61	Ordered Arrays of Dual-Diameter Nanopillars for Maximized Optical Absorption. Nano Letters, 2010, 10, 3823-3827.	9.1	269
62	Photoactuators and motors based on carbon nanotubes with selective chirality distributions. Nature Communications, 2014, 5, 2983.	12.8	269
63	High Photoluminescence Quantum Yield in Band Gap Tunable Bromide Containing Mixed Halide Perovskites. Nano Letters, 2016, 16, 800-806.	9.1	269
64	Strain-engineered growth of two-dimensional materials. Nature Communications, 2017, 8, 608.	12.8	253
65	2D-2D tunneling field-effect transistors using WSe2/SnSe2 heterostructures. Applied Physics Letters, 2016, 108, .	3.3	252
66	Temperature-adaptive radiative coating for all-season household thermal regulation. Science, 2021, 374, 1504-1509.	12.6	251
67	pâ€Type InP Nanopillar Photocathodes for Efficient Solarâ€Driven Hydrogen Production. Angewandte Chemie - International Edition, 2012, 51, 10760-10764.	13.8	245
68	Electrical suppression of all nonradiative recombination pathways in monolayer semiconductors. Science, 2019, 364, 468-471.	12.6	243
69	Integration of suspended carbon nanotube arrays into electronic devices and electromechanical systems. Applied Physics Letters, 2002, 81, 913-915.	3.3	237
70	Metal-catalyzed crystallization of amorphous carbon to graphene. Applied Physics Letters, 2010, 96, .	3.3	234
71	Highly sensitive electronic whiskers based on patterned carbon nanotube and silver nanoparticle composite films. Proceedings of the National Academy of Sciences of the United States of America, 2014, 111, 1703-1707.	7.1	234
72	Regional and correlative sweat analysis using high-throughput microfluidic sensing patches toward decoding sweat. Science Advances, 2019, 5, eaaw9906.	10.3	234

#	Article	IF	CITATIONS
73	Large-scale, heterogeneous integration of nanowire arrays for image sensor circuitry. Proceedings of the United States of America, 2008, 105, 11066-11070.	7.1	233
74	Recombination Kinetics and Effects of Superacid Treatment in Sulfur- and Selenium-Based Transition Metal Dichalcogenides. Nano Letters, 2016, 16, 2786-2791.	9.1	233
75	Dramatic Reduction of Surface Recombination by in Situ Surface Passivation of Silicon Nanowires. Nano Letters, 2011, 11, 2527-2532.	9.1	230
76	Methylxanthine Drug Monitoring with Wearable Sweat Sensors. Advanced Materials, 2018, 30, e1707442.	21.0	226
77	Challenges and prospects of nanopillar-based solar cells. Nano Research, 2009, 2, 829.	10.4	223
78	Highly deformable liquid-state heterojunction sensors. Nature Communications, 2014, 5, 5032.	12.8	221
79	Air Stable p-Doping of WSe <sub>2</sub> by Covalent Functionalization. ACS Nano, 2014, 8, 10808-10814.	14.6	208
80	Electrical contacts to carbon nanotubes down to 1nm in diameter. Applied Physics Letters, 2005, 87, 173101.	3.3	205
81	Efficient and Sustained Photoelectrochemical Water Oxidation by Cobalt Oxide/Silicon Photoanodes with Nanotextured Interfaces. Journal of the American Chemical Society, 2014, 136, 6191-6194.	13.7	204
82	Air-Stable n-Doping of WSe <sub>2</sub> by Anion Vacancy Formation with Mild Plasma Treatment. ACS Nano, 2016, 10, 6853-6860.	14.6	202
83	Flexible Electrochemical Bioelectronics: The Rise of In Situ Bioanalysis. Advanced Materials, 2020, 32, e1902083.	21.0	200
84	Largeâ€Area Compliant Tactile Sensors Using Printed Carbon Nanotube Activeâ€Matrix Backplanes. Advanced Materials, 2015, 27, 1561-1566.	21.0	198
85	Patterned growth of single-walled carbon nanotubes on full 4-inch wafers. Applied Physics Letters, 2001, 79, 4571-4573.	3.3	195
86	Magnesium Fluoride Electron-Selective Contacts for Crystalline Silicon Solar Cells. ACS Applied Materials & Interfaces, 2016, 8, 14671-14677.	8.0	188
87	Miniature Organic Transistors with Carbon Nanotubes as Quasi-One-Dimensional Electrodes. Journal of the American Chemical Society, 2004, 126, 11774-11775.	13.7	184
88	Mid-Wave Infrared Photoconductors Based on Black Phosphorus-Arsenic Alloys. ACS Nano, 2017, 11, 11724-11731.	14.6	184
89	A Fully Integrated and Self-Powered Smartwatch for Continuous Sweat Glucose Monitoring. ACS Sensors, 2019, 4, 1925-1933.	7.8	184
90	A wearable patch for continuous analysis of thermoregulatory sweat at rest. Nature Communications, 2021, 12, 1823.	12.8	181

#	Article	IF	CITATIONS
91	Conductive and Stable Magnesium Oxide Electron‧elective Contacts for Efficient Silicon Solar Cells. Advanced Energy Materials, 2017, 7, 1601863.	19.5	174
92	Hole Contacts on Transition Metal Dichalcogenides: Interface Chemistry and Band Alignments. ACS Nano, 2014, 8, 6265-6272.	14.6	173
93	Application of 3D Printing for Smart Objects with Embedded Electronic Sensors and Systems. Advanced Materials Technologies, 2016, 1, 1600013.	5.8	167
94	Stable Dopant-Free Asymmetric Heterocontact Silicon Solar Cells with Efficiencies above 20%. ACS Energy Letters, 2018, 3, 508-513.	17.4	164
95	Reactive Sputtering of Bismuth Vanadate Photoanodes for Solar Water Splitting. Journal of Physical Chemistry C, 2013, 117, 21635-21642.	3.1	162
96	Ballistic InAs Nanowire Transistors. Nano Letters, 2013, 13, 555-558.	9.1	155
97	Evaporated tellurium thin films for p-type field-effect transistors and circuits. Nature Nanotechnology, 2020, 15, 53-58.	31.5	153
98	Amorphous Si Thin Film Based Photocathodes with High Photovoltage for Efficient Hydrogen Production. Nano Letters, 2013, 13, 5615-5618.	9.1	151
99	Smart Actuators and Adhesives for Reconfigurable Matter. Accounts of Chemical Research, 2017, 50, 691-702.	15.6	151
100	Wafer-Scale, Sub-5 nm Junction Formation by Monolayer Doping and Conventional Spike Annealing. Nano Letters, 2009, 9, 725-730.	9.1	148
101	Large-area and bright pulsed electroluminescence in monolayer semiconductors. Nature Communications, 2018, 9, 1229.	12.8	146
102	Efficient solar-driven electrochemical CO <sub>2</sub> reduction to hydrocarbons and oxygenates. Energy and Environmental Science, 2017, 10, 2222-2230.	30.8	145
103	ELECTRICAL TRANSPORT PROPERTIES AND FIELD EFFECT TRANSISTORS OF CARBON NANOTUBES. Nano, 2006, 01, 1-13.	1.0	142
104	Nanopillar photovoltaics: Materials, processes, and devices. Nano Energy, 2012, 1, 132-144.	16.0	142
105	Room temperature multiplexed gas sensing using chemical-sensitive 3.5-nm-thin silicon transistors. Science Advances, 2017, 3, e1602557.	10.3	142
106	High Luminescence Efficiency in MoS <sub>2</sub> Grown by Chemical Vapor Deposition. ACS Nano, 2016, 10, 6535-6541.	14.6	140
107	Defective TiO2 with high photoconductive gain for efficient and stable planar heterojunction perovskite solar cells. Nature Communications, 2016, 7, 12446.	12.8	139
108	Engineering Light Outcoupling in 2D Materials. Nano Letters, 2015, 15, 1356-1361.	9.1	138

#	Article	IF	CITATIONS
109	Extremely reduced dielectric confinement in two-dimensional hybrid perovskites with large polar organics. Communications Physics, 2018, 1, .	5.3	135
110	Ten- to 50-nm-long quasi-ballistic carbon nanotube devices obtained without complex lithography. Proceedings of the National Academy of Sciences of the United States of America, 2004, 101, 13408-13410.	7.1	134
111	Lithium Fluoride Based Electron Contacts for High Efficiency nâ€Type Crystalline Silicon Solar Cells. Advanced Energy Materials, 2016, 6, 1600241.	19.5	134
112	Actively variable-spectrum optoelectronics with black phosphorus. Nature, 2021, 596, 232-237.	27.8	132
113	Monolithic Integration of Carbon Nanotube Devices with Silicon MOS Technology. Nano Letters, 2004, 4, 123-127.	9.1	131
114	Role of TiO <sub>2</sub> Surface Passivation on Improving the Performance of p-InP Photocathodes. Journal of Physical Chemistry C, 2015, 119, 2308-2313.	3.1	127
115	Tantalum Oxide Electron-Selective Heterocontacts for Silicon Photovoltaics and Photoelectrochemical Water Reduction. ACS Energy Letters, 2018, 3, 125-131.	17.4	127
116	Palladium/silicon nanowire Schottky barrier-based hydrogen sensors. Sensors and Actuators B: Chemical, 2010, 145, 232-238.	7.8	124
117	Wearable Sweat Band for Noninvasive Levodopa Monitoring. Nano Letters, 2019, 19, 6346-6351.	9.1	121
118	Porous Enzymatic Membrane for Nanotextured Glucose Sweat Sensors with High Stability toward Reliable Noninvasive Health Monitoring. Advanced Functional Materials, 2019, 29, 1902521.	14.9	120
119	Electrical properties and devices of large-diameter single-walled carbon nanotubes. Applied Physics Letters, 2002, 80, 1064-1066.	3.3	118
120	Large scale, highly ordered assembly of nanowire parallel arrays by differential roll printing. Applied Physics Letters, 2007, 91, .	3.3	117
121	Uncovering the intrinsic size dependence of hydriding phase transformations in nanocrystals. Nature Materials, 2013, 12, 905-912.	27.5	116
122	19.2% Efficient InP Heterojunction Solar Cell with Electron-Selective TiO <sub>2</sub> Contact. ACS Photonics, 2014, 1, 1245-1250.	6.6	116
123	Monolithic 3D CMOS Using Layered Semiconductors. Advanced Materials, 2016, 28, 2547-2554.	21.0	107
124	General Thermal Texturization Process of MoS <sub>2</sub> for Efficient Electrocatalytic Hydrogen Evolution Reaction. Nano Letters, 2016, 16, 4047-4053.	9.1	106
125	Parallel Array InAs Nanowire Transistors for Mechanically Bendable, Ultrahigh Frequency Electronics. ACS Nano, 2010, 4, 5855-5860.	14.6	105
126	Low-Resistance Electrical Contact to Carbon Nanotubes With Graphitic Interfacial Layer. IEEE Transactions on Electron Devices, 2012, 59, 12-19.	3.0	105

#	Article	IF	CITATIONS
127	3D Printed "Earable―Smart Devices for Real-Time Detection of Core Body Temperature. ACS Sensors, 2017, 2, 990-997.	7.8	105
128	Band Tailing and Deep Defect States in CH <sub>3</sub> NH <sub>3</sub> Pb(I <sub>1–<i>x</i></sub> Br <sub><i>x</i></sub> ) <sub>3</sub> Perovskites As Revealed by Sub-Bandgap Photocurrent. ACS Energy Letters, 2017, 2, 709-715.	17.4	102
129	Wafer-Scale Growth of WSe <sub>2</sub> Monolayers Toward Phase-Engineered Hybrid WO <sub><i>x</i>/sub&gt;/WSe<sub>2</sub> Films with Sub-ppb NO<sub><i>x</i>/sub&gt; Gas Sensing by a Low-Temperature Plasma-Assisted Selenization Process. Chemistry of Materials, 2017, 29, 1587-1598.</sub></sub>	6.7	99
130	Quantum Confinement Effects in Nanoscale-Thickness InAs Membranes. Nano Letters, 2011, 11, 5008-5012.	9.1	97
131	A Low Resistance Calcium/Reduced Titania Passivated Contact for High Efficiency Crystalline Silicon Solar Cells. Advanced Energy Materials, 2017, 7, 1602606.	19.5	97
132	A fully roll-to-roll gravure-printed carbon nanotube-based active matrix for multi-touch sensors. Scientific Reports, 2015, 5, 17707.	3.3	96
133	Regular Arrays of 2 nm Metal Nanoparticles for Deterministic Synthesis of Nanomaterials. Journal of the American Chemical Society, 2005, 127, 11942-11943.	13.7	95
134	Defect passivation of transition metal dichalcogenides via a charge transfer van der Waals interface. Science Advances, 2017, 3, e1701661.	10.3	95
135	MoS2 Heterojunctions by Thickness Modulation. Scientific Reports, 2015, 5, 10990.	3.3	93
136	Si photocathode with Ag-supported dendritic Cu catalyst for CO <sub>2</sub> reduction. Energy and Environmental Science, 2019, 12, 1068-1077.	30.8	93
137	Highly Uniform and Stable n-Type Carbon Nanotube Transistors by Using Positively Charged Silicon Nitride Thin Films. Nano Letters, 2015, 15, 392-397.	9.1	92
138	Efficient Formation of Iron Nanoparticle Catalysts on Silicon Oxide by Hydroxylamine for Carbon Nanotube Synthesis and Electronics. Nano Letters, 2003, 3, 157-161.	9.1	90
139	Chemical Bath Deposition of p-Type Transparent, Highly Conducting (CuS) <sub><i>x</i></sub> :(ZnS) <sub>1–<i>x</i></sub> Nanocomposite Thin Films and Fabrication of Si Heterojunction Solar Cells. Nano Letters, 2016, 16, 1925-1932.	9.1	89
140	Highly Stable Hysteresis-Free Carbon Nanotube Thin-Film Transistors by Fluorocarbon Polymer Encapsulation. ACS Applied Materials & Interfaces, 2014, 6, 8441-8446.	8.0	87
141	Carbon Nanotube Active-Matrix Backplanes for Mechanically Flexible Visible Light and X-ray Imagers. Nano Letters, 2013, 13, 5425-5430.	9.1	86
142	Artificial Photosynthesis on TiO <sub>2</sub> -Passivated InP Nanopillars. Nano Letters, 2015, 15, 6177-6181.	9.1	86
143	Highly Stable Near-Unity Photoluminescence Yield in Monolayer MoS <sub>2</sub> by Fluoropolymer Encapsulation and Superacid Treatment. ACS Nano, 2017, 11, 5179-5185.	14.6	86
144	Glove-based sensors for multimodal monitoring of natural sweat. Science Advances, 2020, 6, eabb8308.	10.3	86

#	Article	IF	CITATIONS
145	Nanoscale InGaSb Heterostructure Membranes on Si Substrates for High Hole Mobility Transistors. Nano Letters, 2012, 12, 2060-2066.	9.1	85
146	Short-Channel Transistors Constructed with Solution-Processed Carbon Nanotubes. ACS Nano, 2013, 7, 798-803.	14.6	83
147	III–V Complementary Metal–Oxide–Semiconductor Electronics on Silicon Substrates. Nano Letters, 2012, 12, 3592-3595.	9.1	80
148	Design constraints and guidelines for CdS/CdTe nanopillar based photovoltaics. Applied Physics Letters, 2010, 96, .	3.3	78
149	Nanoscale Bipolar and Complementary Resistive Switching Memory Based on Amorphous Carbon. IEEE Transactions on Electron Devices, 2011, 58, 3933-3939.	3.0	78
150	Synthetic WSe <sub>2</sub> monolayers with high photoluminescence quantum yield. Science Advances, 2019, 5, eaau4728.	10.3	78
151	BiVO <sub>4</sub> thin film photoanodes grown by chemical vapor deposition. Physical Chemistry Chemical Physics, 2014, 16, 1651-1657.	2.8	77
152	Dopantâ€Free Partial Rear Contacts Enabling 23% Silicon Solar Cells. Advanced Energy Materials, 2019, 9, 1803367.	19.5	77
153	Trace‣evel, Multiâ€Gas Detection for Food Quality Assessment Based on Decorated Silicon Transistor Arrays. Advanced Materials, 2020, 32, e1908385.	21.0	77
154	Ultrathin body InAs tunneling field-effect transistors on Si substrates. Applied Physics Letters, 2011, 98, .	3.3	76
155	Air stable <i>n</i> -doping of WSe2 by silicon nitride thin films with tunable fixed charge density. APL Materials, 2014, 2, .	5.1	76
156	Quantum of optical absorption in two-dimensional semiconductors. Proceedings of the National Academy of Sciences of the United States of America, 2013, 110, 11688-11691.	7.1	75
157	Optical and electrical properties of two-dimensional palladium diselenide. Applied Physics Letters, 2019, 114, .	3.3	74
158	Self-Aligned, Extremely High Frequency III–V Metal-Oxide-Semiconductor Field-Effect Transistors on Rigid and Flexible Substrates. Nano Letters, 2012, 12, 4140-4145.	9.1	73
159	Nanoscale doping of InAs via sulfur monolayers. Applied Physics Letters, 2009, 95, .	3.3	71
160	Near-ideal electrical properties of InAs/WSe2 van der Waals heterojunction diodes. Applied Physics Letters, 2013, 102, .	3.3	71
161	Synthesis, contact printing, and device characterization of Ni-catalyzed, crystalline InAs nanowires. Nano Research, 2008, 1, 32-39.	10.4	70
162	Monolayer Resist for Patterned Contact Printing of Aligned Nanowire Arrays. Journal of the American Chemical Society, 2009, 131, 2102-2103.	13.7	70

#	Article	IF	CITATIONS
163	A Wearable Nutrition Tracker. Advanced Materials, 2021, 33, e2006444.	21.0	70
164	Black Ge Based on Crystalline/Amorphous Core/Shell Nanoneedle Arrays. Nano Letters, 2010, 10, 520-523.	9.1	68
165	Increasing Photoluminescence Quantum Yield by Nanophotonic Design of Quantum-Confined Halide Perovskite Nanowire Arrays. Nano Letters, 2019, 19, 2850-2857.	9.1	67
166	Observation of Degenerate One-Dimensional Sub-Bands in Cylindrical InAs Nanowires. Nano Letters, 2012, 12, 1340-1343.	9.1	65
167	A direct thin-film path towards low-cost large-area III-V photovoltaics. Scientific Reports, 2013, 3, 2275.	3.3	65
168	Cation-Dependent Light-Induced Halide Demixing in Hybrid Organic–Inorganic Perovskites. Nano Letters, 2018, 18, 3473-3480.	9.1	65
169	Electrical Properties of Synthesized Large-Area MoS2 Field-Effect Transistors Fabricated with Inkjet-Printed Contacts. ACS Nano, 2016, 10, 2819-2826.	14.6	64
170	Neutral Exciton Diffusion in Monolayer MoS <sub>2</sub> . ACS Nano, 2020, 14, 13433-13440.	14.6	62
171	Formation and Characterization of NixInAs/InAs Nanowire Heterostructures by Solid Source Reaction. Nano Letters, 2008, 8, 4528-4533.	9.1	61
172	Prospect of tunneling green transistor for 0.1V CMOS. , 2010, , .		61
173	Fully printed flexible and disposable wireless cyclic voltammetry tag. Scientific Reports, 2015, 5, 8105.	3.3	61
174	Design of Surfactant–Substrate Interactions for Roll-to-Roll Assembly of Carbon Nanotubes for Thin-Film Transistors. Journal of the American Chemical Society, 2014, 136, 11188-11194.	13.7	60
175	Calcium contacts to nâ€ŧype crystalline silicon solar cells. Progress in Photovoltaics: Research and Applications, 2017, 25, 636-644.	8.1	60
176	Hybrid Coreâ^'Shell Nanowire Forests as Self-Selective Chemical Connectors. Nano Letters, 2009, 9, 2054-2058.	9.1	59
177	Strong optical response and light emission from a monolayer molecular crystal. Nature Communications, 2019, 10, 5589.	12.8	59
178	Roll-to-Roll Anodization and Etching of Aluminum Foils for High-Throughput Surface Nanotexturing. Nano Letters, 2011, 11, 3425-3430.	9.1	58
179	Contact printing of compositionally graded CdS <sub><i>x</i></sub> Se <sub>1â°<i>x</i></sub> Se <sub>11°<i>x</i></sub> snanowire parallel arrays for tunable photodetectors. Nanotechnology, 2012, 23, 045201.	2.6	58
180	Patterned p-Doping of InAs Nanowires by Gas-Phase Surface Diffusion of Zn. Nano Letters, 2010, 10, 509-513.	9.1	57

#	Article	IF	CITATIONS
181	Room Temperature Oxide Deposition Approach to Fully Transparent, Allâ€Oxide Thinâ€Film Transistors. Advanced Materials, 2015, 27, 6090-6095.	21.0	57
182	A multi-modal sweat sensing patch for cross-verification of sweat rate, total ionic charge, and Na <sup>+</sup> concentration. Lab on A Chip, 2019, 19, 3179-3189.	6.0	56
183	Physical and Chemical Sensing With Electronic Skin. Proceedings of the IEEE, 2019, 107, 2155-2167.	21.3	56
184	Wearable Biosensors for Body Computing. Advanced Functional Materials, 2021, 31, 2008087.	14.9	56
185	Molecular monolayers for conformal, nanoscale doping of InP nanopillar photovoltaics. Applied Physics Letters, 2011, 98, .	3.3	54
186	Solutionâ€Processed Transparent Selfâ€Powered pâ€CuSâ€ZnS/nâ€ZnO UV Photodiode. Physica Status Solidi - Rapid Research Letters, 2018, 12, 1700381.	2.4	54
187	Electron-Selective TiO2 Contact for Cu(In,Ga)Se2 Solar Cells. Scientific Reports, 2015, 5, 16028.	3.3	52
188	Enhanced Photocatalytic Reduction of CO <sub>2</sub> to CO through TiO <sub>2</sub> Passivation of InP in Ionic Liquids. Chemistry - A European Journal, 2015, 21, 13502-13507.	3.3	52
189	Inhibited nonradiative decay at all exciton densities in monolayer semiconductors. Science, 2021, 373, 448-452.	12.6	52
190	Spin-On Organic Polymer Dopants for Silicon. Journal of Physical Chemistry Letters, 2013, 4, 3741-3746.	4.6	51
191	Substrate-Dependent Exciton Diffusion and Annihilation in Chemically Treated MoS <sub>2</sub> and WS <sub>2</sub> . Journal of Physical Chemistry C, 2020, 124, 12175-12184.	3.1	51
192	Recycling Is Not Always Good: The Dangers of Self-Plagiarism. ACS Nano, 2012, 6, 1-4.	14.6	49
193	Evaporated Se <i><sub>x</sub></i> Te <sub>1â€</sub> <i><sub>x</sub></i> Thin Films with Tunable Bandgaps for Shortâ€Wave Infrared Photodetectors. Advanced Materials, 2020, 32, e2001329.	21.0	49
194	Fully R2Râ€Printed Carbonâ€Nanotubeâ€Based Limitless Length of Flexible Activeâ€Matrix for Electrophoretic Display Application. Advanced Electronic Materials, 2020, 6, 1901431.	5.1	49
195	The 2008 Kavli Prize in Nanoscience: Carbon Nanotubes. ACS Nano, 2008, 2, 1329-1335.	14.6	48
196	Nicotine Monitoring with a Wearable Sweat Band. ACS Sensors, 2020, 5, 1831-1837.	7.8	48
197	Performance Enhancement of a Graphene-Zinc Phosphide Solar Cell Using the Electric Field-Effect. Nano Letters, 2014, 14, 4280-4285.	9.1	45
198	Direct growth of single-crystalline III–V semiconductors on amorphous substrates. Nature Communications, 2016, 7, 10502.	12.8	45

#	Article	IF	CITATIONS
199	Flexible Carbonâ€Nanofiber Connectors with Anisotropic Adhesion Properties. Small, 2010, 6, 22-26.	10.0	44
200	Intrinsic Optoelectronic Characteristics of MoS <sub>2</sub> Phototransistors <i>via</i> a Fully Transparent van der Waals Heterostructure. ACS Nano, 2019, 13, 9638-9646.	14.6	43
201	Nanoscale Semiconductor "X―on Substrate "Y―– Processes, Devices, and Applications. Advanced Materials, 2011, 23, 3115-3127.	21.0	42
202	Quantum Size Effects on the Chemical Sensing Performance of Two-Dimensional Semiconductors. Journal of Physical Chemistry C, 2012, 116, 9750-9754.	3.1	41
203	Highly Sensitive Bulk Silicon Chemical Sensors with Sub-5 nm Thin Charge Inversion Layers. ACS Nano, 2018, 12, 2948-2954.	14.6	41
204	Benchmarking the performance of ultrathin body InAs-on-insulator transistors as a function of body thickness. Applied Physics Letters, 2011, 99, .	3.3	40
205	Superacid-Treated Silicon Surfaces: Extending the Limit of Carrier Lifetime for Photovoltaic Applications. IEEE Journal of Photovoltaics, 2017, 7, 1574-1583.	2.5	40
206	Multifunctional, flexible electronic systems based on engineered nanostructured materials. Nanotechnology, 2012, 23, 344001.	2.6	38
207	Integrated Manufacture of Exoskeletons and Sensing Structures for Folded Millirobots. Journal of Mechanisms and Robotics, 2015, 7, .	2.2	38
208	Superacid Passivation of Crystalline Silicon Surfaces. ACS Applied Materials & Interfaces, 2016, 8, 24205-24211.	8.0	38
209	Phosphine Oxide Monolayers on SiO <sub>2</sub> Surfaces. Angewandte Chemie - International Edition, 2008, 47, 4440-4442.	13.8	37
210	Solar cells on curtains. Nature Materials, 2008, 7, 835-836.	27.5	37
211	Fermi level stabilization and band edge energies in CdxZn1â^'xO alloys. Journal of Applied Physics, 2014, 115, .	2.5	37
212	Temperature and Humidity Stable Alkali/Alkalineâ€Earth Metal Carbonates as Electron Heterocontacts for Silicon Photovoltaics. Advanced Energy Materials, 2018, 8, 1800743.	19.5	35
213	Polymeric Electron-Selective Contact for Crystalline Silicon Solar Cells with an Efficiency Exceeding 19%. ACS Energy Letters, 2020, 5, 897-902.	17.4	35
214	High quality interfaces of InAs-on-insulator field-effect transistors with ZrO2 gate dielectrics. Applied Physics Letters, 2013, 102, .	3.3	33
215	Nonepitaxial Thin-Film InP for Scalable and Efficient Photocathodes. Journal of Physical Chemistry Letters, 2015, 6, 2177-2182.	4.6	33
216	Deterministic Nucleation of InP on Metal Foils with the Thin-Film Vapor–Liquid–Solid Growth Mode. Chemistry of Materials, 2014, 26, 1340-1344.	6.7	32

#	Article	IF	CITATIONS
217	Highly Reliable Superhydrophobic Protection for Organic Field-Effect Transistors by Fluoroalkylsilane-Coated TiO <sub>2</sub> Nanoparticles. ACS Nano, 2018, 12, 11062-11069.	14.6	32
218	Tellurium Singleâ€Crystal Arrays by Lowâ€Temperature Evaporation and Crystallization. Advanced Materials, 2021, 33, e2100860.	21.0	32
219	Wet and Dry Adhesion Properties of Selfâ€Selective Nanowire Connectors. Advanced Functional Materials, 2009, 19, 3098-3102.	14.9	31
220	Hierarchical polymer micropillar arrays decorated with ZnO nanowires. Nanotechnology, 2010, 21, 295305.	2.6	30
221	Comparative study of solution-processed carbon nanotube network transistors. Applied Physics Letters, 2012, 101, 112104.	3.3	30
222	Thermoresponsive Chemical Connectors Based on Hybrid Nanowire Forests. Angewandte Chemie - International Edition, 2010, 49, 616-619.	13.8	29
223	Shape-Controlled Synthesis of Single-Crystalline Nanopillar Arrays by Template-Assisted Vaporâ^'Liquidâ^'Solid Process. Journal of the American Chemical Society, 2010, 132, 13972-13974.	13.7	29
224	Improved photoswitching response times of MoS2 field-effect transistors by stacking <i>p</i> -type copper phthalocyanine layer. Applied Physics Letters, 2016, 109, .	3.3	29
225	Long-Wave Infrared Photodetectors Based on 2D Platinum Diselenide atop Optical Cavity Substrates. ACS Nano, 2021, 15, 6573-6581.	14.6	29
226	Hybrid core-multishell nanowire forests for electrical connector applications. Applied Physics Letters, 2009, 94, 263110.	3.3	28
227	Ultrathin-Body High-Mobility InAsSb-on-Insulator Field-Effect Transistors. IEEE Electron Device Letters, 2012, 33, 504-506.	3.9	28
228	Dip Coating Passivation of Crystalline Silicon by Lewis Acids. ACS Nano, 2019, 13, 3723-3729.	14.6	28
229	Rationally Designed, Threeâ€Dimensional Carbon Nanotube Backâ€Contacts for Efficient Solar Devices. Advanced Energy Materials, 2011, 1, 1040-1045.	19.5	27
230	Vertically aligned tungsten oxide nanorod film with enhanced performance in photoluminescence humidity sensing. Sensors and Actuators B: Chemical, 2014, 202, 708-713.	7.8	27
231	Scanning Probe Lithography Patterning of Monolayer Semiconductors and Application in Quantifying Edge Recombination. Advanced Materials, 2019, 31, e1900136.	21.0	27
232	Elimination of Response to Relative Humidity Changes in Chemical-Sensitive Field-Effect Transistors. ACS Sensors, 2019, 4, 1857-1863.	7.8	24
233	Generic Nanomaterial Positioning by Carrier and Stationary Phase Design. Nano Letters, 2007, 7, 2764-2768.	9.1	23
234	Nanoscale Structural Engineering via Phase Segregation: Auâ^'Ge System. Nano Letters, 2010, 10, 393-397.	9.1	23

#	Article	IF	CITATIONS
235	Strain engineering of epitaxially transferred, ultrathin layers of III-V semiconductor on insulator. Applied Physics Letters, 2011, 98, 012111.	3.3	23
236	Determining Atomic-Scale Structure and Composition of Organo-Lead Halide Perovskites by Combining High-Resolution X-ray Absorption Spectroscopy and First-Principles Calculations. ACS Energy Letters, 2017, 2, 1183-1189.	17.4	23
237	Spatially Precise Transfer of Patterned Monolayer WS <sub>2</sub> and MoS <sub>2</sub> with Features Larger than 10 <sup>4</sup> μm <sup>2</sup> Directly from Multilayer Sources. ACS Applied Electronic Materials, 2019, 1, 407-416.	4.3	23
238	A generic electroluminescent device for emission from infrared to ultraviolet wavelengths. Nature Electronics, 2020, 3, 612-621.	26.0	23
239	Mid- to long-wave infrared computational spectroscopy with a graphene metasurface modulator. Scientific Reports, 2020, 10, 5377.	3.3	23
240	Resettable Microfluidics for Broad-Range and Prolonged Sweat Rate Sensing. ACS Sensors, 2022, 7, 1156-1164.	7.8	23
241	Nanoscience and Nanotechnology Impacting Diverse Fields of Science, Engineering, and Medicine. ACS Nano, 2016, 10, 10615-10617.	14.6	22
242	Nanoscale Junction Formation by Gas-Phase Monolayer Doping. ACS Applied Materials & Interfaces, 2017, 9, 20648-20655.	8.0	22
243	Anomalously Suppressed Thermal Conduction by Electronâ€Phonon Coupling in Chargeâ€Đensityâ€Wave Tantalum Disulfide. Advanced Science, 2020, 7, 1902071.	11.2	22
244	High optical quality polycrystalline indium phosphide grown on metal substrates by metalorganic chemical vapor deposition. Journal of Applied Physics, 2012, 111, 123112.	2.5	21
245	Enhanced Nearâ€Bandgap Response in InP Nanopillar Solar Cells. Advanced Energy Materials, 2014, 4, 1400061.	19.5	21
246	Oriented Growth of Gold Nanowires on MoS <sub>2</sub> . Advanced Functional Materials, 2015, 25, 6257-6264.	14.9	21
247	Compliant substrate epitaxy: Au on <mml:math xmlns:mml="http://www.w3.org/1998/Math/MathML"&gt;<mml:msub><mml:mi>MoS</mml:mi><mml:mn>2Physical Review B, 2016, 93, .</mml:mn></mml:msub></mml:math 	:m <b>a.</b> 2 <td>nl:msub&gt;</td>	nl:msub>
248	Origin of multi-level switching and telegraphic noise in organic nanocomposite memory devices. Scientific Reports, 2016, 6, 33967.	3.3	21
249	Extreme In-Plane Thermal Conductivity Anisotropy in Titanium Trisulfide Caused by Heat-Carrying Optical Phonons. Nano Letters, 2020, 20, 5221-5227.	9.1	21
250	Wearable sweat biosensors. , 2016, , .		20
251	Illâ€Vs at scale: a PV manufacturing cost analysis of the thin film vapor–liquid–solid growth mode. Progress in Photovoltaics: Research and Applications, 2016, 24, 871-878.	8.1	20
252	Centimeterâ€ <b>5</b> cale and Visible Wavelength Monolayer Lightâ€Emitting Devices. Advanced Functional Materials, 2020, 30, 1907941.	14.9	20

#	Article	IF	CITATIONS
253	Universal Inverse Scaling of Exciton–Exciton Annihilation Coefficient with Exciton Lifetime. Nano Letters, 2021, 21, 424-429.	9.1	20
254	Light–Matter Interaction Enhancement in Anisotropic 2D Black Phosphorus via Polarization-Tailoring Nano-Optics. ACS Photonics, 2021, 8, 1120-1128.	6.6	20
255	Surface Charge Transfer Doping of Ill–V Nanostructures. Journal of Physical Chemistry C, 2013, 117, 17845-17849.	3.1	19
256	Quantum Well InAs/AlSb/GaSb Vertical Tunnel FET With HSQ Mechanical Support. IEEE Nanotechnology Magazine, 2015, 14, 580-584.	2.0	19
257	Fully gravure printed complementary carbon nanotube TFTs for a clock signal generator using an epoxy-imine based cross-linker as an n-dopant and encapsulant. Nanoscale, 2016, 8, 19876-19881.	5.6	19
258	Measuring the Edge Recombination Velocity of Monolayer Semiconductors. Nano Letters, 2017, 17, 5356-5360.	9.1	19
259	Zirconium oxide surface passivation of crystalline silicon. Applied Physics Letters, 2018, 112, .	3.3	19
260	Bright Mid-Wave Infrared Resonant-Cavity Light-Emitting Diodes Based on Black Phosphorus. Nano Letters, 2022, 22, 1294-1301.	9.1	19
261	Morphological and spatial control of InP growth using closed-space sublimation. Journal of Applied Physics, 2012, 112, 123102.	2.5	18
262	Transistorâ€Based Workâ€Function Measurement of Metal–Organic Frameworks for Ultra‣owâ€Power, Rationally Designed Chemical Sensors. Chemistry - A European Journal, 2019, 25, 13176-13183.	3.3	18
263	Engineering Exciton Recombination Pathways in Bilayer WSe <sub>2</sub> for Bright Luminescence. ACS Nano, 2022, 16, 1339-1345.	14.6	18
264	Influence of catalyst choices on transport behaviors of InAs NWs for high-performance nanoscale transistors. Physical Chemistry Chemical Physics, 2013, 15, 2654.	2.8	17
265	Ultrafast Spontaneous Emission from a Slot-Antenna Coupled WSe <sub>2</sub> Monolayer. ACS Photonics, 2018, 5, 2701-2705.	6.6	17
266	Development of a compact neutron source based on field ionization processes. Journal of Vacuum Science and Technology B:Nanotechnology and Microelectronics, 2011, 29, 02B107.	1.2	16
267	Two-dimensional to three-dimensional tunneling in InAs/AISb/GaSb quantum well heterojunctions. Journal of Applied Physics, 2013, 114, .	2.5	16
268	Electrodeposition of High-Purity Indium Thin Films and Its Application to Indium Phosphide Solar Cells. Journal of the Electrochemical Society, 2014, 161, D794-D800.	2.9	16
269	Thermal Stability of Hole-Selective Tungsten Oxide: In Situ Transmission Electron Microscopy Study. Scientific Reports, 2018, 8, 12651.	3.3	16
270	Integration of amorphous ferromagnetic oxides with multiferroic materials for room temperature magnetoelectric spintronics. Scientific Reports, 2020, 10, 3583.	3.3	16

#	Article	IF	CITATIONS
271	Photovoltaic Material Characterization With Steady State and Transient Photoluminescence. IEEE Journal of Photovoltaics, 2015, 5, 282-287.	2.5	15
272	Carbon Nanotubes: From Growth, Placement and Assembly Control to 60mV/decade and Sub-60 mV/decade Tunnel Transistors. , 2006, , .		14
273	A compact neutron generator using a field ionization source. Review of Scientific Instruments, 2012, 83, 02B312.	1.3	14
274	Analysis of the interface characteristics of CVD-grown monolayer MoS <sub>2</sub> by noise measurements. Nanotechnology, 2017, 28, 145702.	2.6	14
275	Thinâ€Film Solar Cells with InP Absorber Layers Directly Grown on Nonepitaxial Metal Substrates. Advanced Energy Materials, 2015, 5, 1501337.	19.5	13
276	Bright electroluminescence in ambient conditions from WSe2 p-n diodes using pulsed injection. Applied Physics Letters, 2019, 115, 011103.	3.3	13
277	Survey of dopant-free carrier-selective contacts for silicon solar cells. , 2016, , .		12
278	Increased Optoelectronic Quality and Uniformity of Hydrogenated p-InP Thin Films. Chemistry of Materials, 2016, 28, 4602-4607.	6.7	12
279	Thermal stability for Te-based devices. Applied Physics Letters, 2020, 117, .	3.3	12
280	Deterministic Assembly of Arrays of Lithographically Defined WS2 and MoS2 Monolayer Features Directly From Multilayer Sources Into Van Der Waals Heterostructures. Journal of Micro and Nano-Manufacturing, 2019, 7, .	0.7	12
281	Effects of palladium coating on field-emission properties of carbon nanofibers in a hydrogen plasma. Thin Solid Films, 2013, 534, 488-491.	1.8	11
282	Performance Limits of an Alternating Current Electroluminescent Device. Advanced Materials, 2021, 33, e2005635.	21.0	11
283	Enhanced Neutral Exciton Diffusion in Monolayer WS <sub>2</sub> by Exciton–Exciton Annihilation. ACS Nano, 2022, 16, 8005-8011.	14.6	11
284	Efficiency Roll-Off Free Electroluminescence from Monolayer WSe <sub>2</sub> . Nano Letters, 2022, 22, 5316-5321.	9.1	11
285	InAs FinFETs Performance Enhancement by Superacid Surface Treatment. IEEE Transactions on Electron Devices, 2019, 66, 1856-1861.	3.0	10
286	Molecular Materials with Short Radiative Lifetime for High-Speed Light-Emitting Devices. Matter, 2020, 3, 1832-1844.	10.0	10
287	Copper Tetracyanoquinodimethane (CuTCNQ): A Metal–Organic Semiconductor for Room-Temperature Visible to Long-Wave Infrared Photodetection. ACS Applied Materials & Interfaces, 2021, 13, 38544-38552.	8.0	10
288	A Resonantly Driven, Electroluminescent Metal Oxide Semiconductor Capacitor with High Power Efficiency. ACS Nano, 2021, 15, 15210-15217.	14.6	10

4

#	Article	IF	CITATIONS
289	2D layered materials: From materials properties to device applications. , 2015, , .		9
290	PCBM-Grafted MWNT for Enhanced Electron Transport in Polymer Solar Cells. Journal of the Electrochemical Society, 2011, 158, A237.	2.9	8
291	Carbon Nanotubes: Printed Carbon Nanotube Electronics and Sensor Systems (Adv. Mater. 22/2016). Advanced Materials, 2016, 28, 4396-4396.	21.0	8
292	Microchannel contacting of crystalline silicon solar cells. Scientific Reports, 2017, 7, 9085.	3.3	8
293	High-gain monolithic 3D CMOS inverter using layered semiconductors. Applied Physics Letters, 2017, 111, .	3.3	8
294	Shape-controlled single-crystal growth of InP at low temperatures down to 220 ŰC. Proceedings of the United States of America, 2020, 117, 902-906.	7.1	8
295	Wearable Biosensors for Body Computing (Adv. Funct. Mater. 39/2021). Advanced Functional Materials, 2021, 31, 2170290.	14.9	8
296	Flexible Electronics: Flexible Electrochemical Bioelectronics: The Rise of In Situ Bioanalysis (Adv.) Tj ETQq0 0 0 rgI	3T /Overloo 21.0	ck 10 Tf 50 4
297	Orientated Growth of Ultrathin Tellurium by van der Waals Epitaxy. Advanced Materials Interfaces, 2022, 9, .	3.7	7
298	A Year for Nanoscience. ACS Nano, 2014, 8, 11901-11903.	14.6	6
299	Wearable Devices: Wearable Microfluidic Diaphragm Pressure Sensor for Health and Tactile Touch Monitoring (Adv. Mater. 39/2017). Advanced Materials, 2017, 29, .	21.0	6
300	Gate Quantum Capacitance Effects in Nanoscale Transistors. Nano Letters, 2019, 19, 7130-7137.	9.1	6
301	In Situ Transmission Electron Microscopy Study of Molybdenum Oxide Contacts for Silicon Solar Cells. Physica Status Solidi (A) Applications and Materials Science, 2019, 216, 1800998.	1.8	6
302	Graphitic interfacial layer to carbon nanotube for low electrical contact resistance. , 2010, , .		5

303	Be Critical but Fair. ACS Nano, 2013, 7, 8313-8316.	14.6	5
304	Mimicking the Human Brain and More: New Grand Challenge Initiatives. ACS Nano, 2015, 9, 10533-10536.	14.6	5
305	Improved Hydrogen Sensitivity and Selectivity in PdO with Metal-Organic Framework Membrane. Journal of the Electrochemical Society, 2020, 167, 147503.	2.9	5

306 Monolayer doping and diameter-dependent electron mobility assessment of nanowires. , 2009, , .

#	Article	IF	CITATIONS
307	Resistive switching of carbon-based RRAM with CNT electrodes for ultra-dense memory. , 2010, , .		4
308	Photoluminescence imaging characterization of thin-film InP. , 2015, , .		4
309	Nanoscience and Nanotechnology Cross Borders. ACS Nano, 2017, 11, 1123-1126.	14.6	4
310	Power surfing on waves. Nature, 2011, 472, 304-305.	27.8	3
311	We Take It Personally. ACS Nano, 2012, 6, 10417-10419.	14.6	3
312	Grand Plans for Nano. ACS Nano, 2015, 9, 11503-11505.	14.6	3
313	Enhanced Spontaneous Emission from an Optical Antenna Coupled WSe2 Monolayer. , 2015, , .		3
314	Preface to Special Topic: Selected Papers from the International Conference on Flexible and Printed Electronics, Jeju Island, Korea, 2009. Journal of Applied Physics, 2010, 108, 102701.	2.5	2
315	Measuring Academic Impact. ACS Nano, 2012, 6, 6529-6529.	14.6	2
316	Series resistance and mobility in mechanically-exfoliated layered transition metal dichalcogenide MOSFETs. , 2014, , .		2
317	Two-Chip Wireless H2S Gas Sensor System Requiring Zero Additional Electronic Components. , 2019, , .		2
318	Laserâ€Assisted Thermomechanical Thinning of MoTe <sub>2</sub> in Nanoscale Lateral Resolution. Advanced Materials Interfaces, 2022, 9, .	3.7	2
319	Self-aligned 40-nm channel carbon nanotube field-effect transistors with subthreshold swings down to 70 mV/decade. , 2005, , .		1
320	Carbon Nanotube Field-Effect Transistors. Integrated Circuits and Systems, 2009, , 63-86.	0.2	1
321	Exciting Times for Nano. ACS Nano, 2013, 7, 10437-10439.	14.6	1
322	Catalyst-dependent morphological evolution by interfacial stress in crystalline–amorphous core–shell germanium nanowires. RSC Advances, 2015, 5, 28454-28459.	3.6	1
323	A Big Year Ahead for Nano in 2018. ACS Nano, 2017, 11, 11755-11757.	14.6	1
324	2D Semiconductor Optoelectropics 2017		1

#	Article	IF	CITATIONS
325	23% efficient n-type crystalline silicon solar cells with passivated partial rear contacts. , 2018, , .		1
326	Growing Contributions of Nano in 2020. ACS Nano, 2020, 14, 16163-16164.	14.6	1
327	Ordered polymer-based spin-on dopants. , 2019, , .		1
328	Theory of liquid-mediated strain release in two-dimensional materials. Physical Review Materials, 2022, 6, .	2.4	1
329	Structural heterogeneity in non-crystalline Te <sub><i>x</i></sub> Se1â^x thin films. Applied Physics Letters, 2022, 121, 012101.	3.3	1
330	Nanowire-based 2-D and 3-D XoY electronics. , 2010, , .		0
331	ACS Nano in 2011 and Looking Forward to 2012. ACS Nano, 2011, 5, 9301-9302.	14.6	Ο
332	Strongly enhanced minority lifetimes in single silicon nanowires by surface passivation. , 2011, , .		0
333	Quantum membranes: A new materials platform for future electronics. , 2013, , .		0
334	Carbon nanotube macroelectronics: toward system-on-plastic. Proceedings of SPIE, 2013, , .	0.8	0
335	Solar fuels production by artificial photosynthesis. , 2013, , .		Ο
336	Frontispiece: Enhanced Photocatalytic Reduction of CO2to CO through TiO2Passivation of InP in Ionic Liquids. Chemistry - A European Journal, 2015, 21, n/a-n/a.	3.3	0
337	Low Pressure Vapor-assisted Solution Process for Tunable Band Gap Pinhole-free Methylammonium Lead Halide Perovskite Films. Journal of Visualized Experiments, 2017, , .	0.3	0
338	Our First and Next Decades at ACS Nano. ACS Nano, 2017, 11, 7553-7555.	14.6	0
339	Measuring the edge recombination velocity of monolayer semiconductors. , 2017, , .		0
340	Investigation of InP defect characteristics grown using novel TF-VLS technique. , 2017, , .		0
341	Metal Nanoparticle Hole Contacts for Silicon Solar Cells. , 2017, , .		0
342	Helmuth Möhwald (1946–2018). ACS Nano, 2018, 12, 3053-3055.	14.6	0

#	Article	IF	CITATIONS
343	Transmission Electron Microscopy Studies of Transition Metal Oxides Employed as Carrier Selective Contacts in Silicon Solar Cells. , 2018, , .		0
344	Scalable Ultra Low-Power Chemical Sensing with Metal-Organic Frameworks. , 2019, , .		0
345	In Situ Transmission Electron Microscopy: A Powerful Tool for the Characterization of Carrier-Selective Contacts. , 2019, , .		0
346	Monolayer Semiconductors: Scanning Probe Lithography Patterning of Monolayer Semiconductors and Application in Quantifying Edge Recombination (Adv. Mater. 48/2019). Advanced Materials, 2019, 31, 1970340.	21.0	0
347	Polarization-Converting Plasmonic Nanoantennas for Light Absorption Enhancement in Anisotropic 2D Black Phosphorus. , 2021, , .		0
348	Longwave Infrared Photoresponse in Copper 7,7,8,8-tetracyano-2,3,5,6-tetraflouroquinodimethane (CuTCNQF4). , 2021, , .		0
349	Bright Electroluminescence from Back-Gated WSe2 P-N Junctions Using Pulsed Injection. , 2018, , .		0
350	Mid-Infrared Computational Spectroscopy with an Electrically-Tunable Graphene Metasurface. , 2019, , $\cdot$		0
351	Long-Wave Infrared Photodetectors Based on Platinum Diselenide. , 2020, , .		0
352	Visible to Long-Wave Infrared Photodetectors based on Copper Tetracyanoquinodimethane (CuTCNQ) Crystals. , 2020, , .		0
353	Tanks and Truth. ACS Nano, 2022, 16, 4975-4976.	14.6	0